JACS
JOURNAL OF THE AMERICAN CHEMICAL SOCIETY
Article
pubs.acs.org/JACS

Rapid Bioorthogonal Chemistry Turn-on through Enzymatic or Long Wavelength Photocatalytic Activation of Tetrazine Ligation

Han Zhang,[†,§] William S. Trout,[†,§] Shuang Liu,[‡] Gabriel A. Andrade,[†] Devin A. Hudson,[†] Samuel L. Scinto,[†] Kevin T. Dicker,[‡] Yi Li,[†] Nikifar Lazouski,[†] Joel Rosenthal,[†] Colin Thorpe,[†] Xinqiao Jia,[‡] and Joseph M. Fox*[,†,‡]

[†]Department of Chemistry and Biochemistry, University of Delaware, Newark, Delaware 19716, United States
[‡]Department of Materials Science and Engineering, University of Delaware, Newark, Delaware 19716, United States

Ⓦ *Web-Enhanced Feature* Ⓢ *Supporting Information*

ABSTRACT: Rapid bioorthogonal reactivity can be induced by controllable, catalytic stimuli using air as the oxidant. Methylene blue (4 μM) irradiated with red light (660 nm) catalyzes the rapid oxidation of a dihydrotetrazine to a tetrazine thereby turning on reactivity toward *trans*-cyclooctene dienophiles. Alternately, the aerial oxidation of dihydrotetrazines can be efficiently catalyzed by nanomolar levels of horseradish peroxidase under peroxide-free conditions. Selection of dihydrotetrazine/tetrazine pairs of sufficient kinetic stability in aerobic aqueous solutions is key to the success of these approaches. In this work, polymer fibers carrying latent dihydrotetrazines were catalytically activated and covalently modified by *trans*-cyclooctene conjugates of small molecules, peptides, and proteins. In addition to visualization with fluorophores, fibers conjugated to a cell adhesive peptide exhibited a dramatically increased ability to mediate contact guidance of cells.

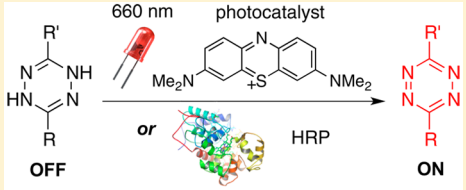

activation in air within minutes using red light or HRP enables instantaneous bioorthogonal labeling

INTRODUCTION

Bioorthogonal chemistry has evolved into a field with broad-reaching applications in biology, medicine, and materials science.[1−4] Driving the field has been the vigorous development of unnatural transformations that proceed selectively in the presence of Nature's functional groups.[5−12] Recently, bioorthogonal chemistry has been utilized in payload release strategies, with the aim of triggering diverse events including drug delivery, gene expression, and modulating materials properties.[13−15] There has also been a growing interest in using external stimuli to induce bioorthogonal reactivity. In particular, photoinducible reactions have emerged as a method for turning on bioorthogonal reactions with temporal and spatial control.[9,16] Key advances include tetrazole[10] and cyclopropenone[11] based ligations, where photolysis produces reactive nitrile imines and cyclooctyne derivatives, respectively. Such "photoclick" reactions generally utilize short-wavelength light to unleash more reactive species.[10,11] The direct use of red or near IR light to induce bioorthogonal reactivity has not been described. Lin has recently described two-photon based photoinducible tetrazole reactions that utilize near-IR light,[8] and Popik has shown that cyclopropenones can be photodecarbonylated by a two-photon process.[17] While two-photon methods provide high spatial resolution,[18] their very small focal volumes currently limit many practical applications. Recently, near-IR photodecaging strategies have been described based on cyanine,[19] BODIPY,[20] and phthalocyanine[21] dyes.[22] A current challenge for red- and near-IR photodecaging strategies lies in the need to improve the kinetics of photorelease.

Enzymatic catalysis presents intriguing additional possibilities for turning on bioorthogonal reactivity. Proteins have been engineered with unnatural side chains capable of bioorthogonal coupling,[2] Recently, bioorthogonal enzymatic decaging has been described in which engineered P450 proteins catalyze reactions to release alcohols.[23] However, the use of an enzyme to create a bioorthogonal coupling partner had not been described. We considered that the enzyme horseradish peroxidase (HRP) might be an effective catalyst for the creation of compounds for bioorthogonal reactivity. HRP finds broad utility in biological assays by oxidizing phenols and other organic substrates.[24] While H_2O_2 is typically required as the terminal oxidant, HRP can oxidize certain substrates (e.g., indole-3-acetic acid, NADH, and hydroquinones) in the absence of peroxide.[25−28]

The inverse-electron demand Diels−Alder reaction of *s*-tetrazines with alkene or alkyne dienophiles, referred to as tetrazine ligation, has emerged as an important reaction in the bioorthogonal toolbox.[29−31] A notable aspect of tetrazine ligations are the exceptionally high rates of reactivity that can be achieved.[31] With strained *trans*-cyclooctenes, we have measured bimolecular rate constants as high as 3.3×10^6 M^{-1} s^{-1} in reactions with tetrazines (Tz), representing the fastest bioorthogonal reactions reported to date.[32,33] Tetrazines are typically synthesized through the chemical oxidation of dihydrotetrazine (DHTz) precursors,[34] and the electroactivity

Received: February 27, 2016
Published: April 14, 2016

DOI: 10.1021/jacs.6b02168
J. Am. Chem. Soc. 2016, 138, 5978−5983

of tetrazines is well established.[35] Recently, Devaraj has demonstrated that electrochemistry can be used to control the redox state of pendant DHTz/Tz groups on the surface of microelectrodes, allowing selective bioconjugation to oxidized electrode surfaces.[36] DHTz-containing metal organic frameworks have also been used as colorimetric materials for the detection of nitrous gases.[37]

Described herein are the first examples of *catalytic* turn-on of the tetrazine ligation, where rapid bioorthogonal reactivity can be induced by a controllable, catalytic stimulus (Figure 1A). Either visible light and a photosensitizer or very low loadings of horseradish peroxidase can be used to catalyze the oxidation of a dihydrotetrazine to a tetrazine.

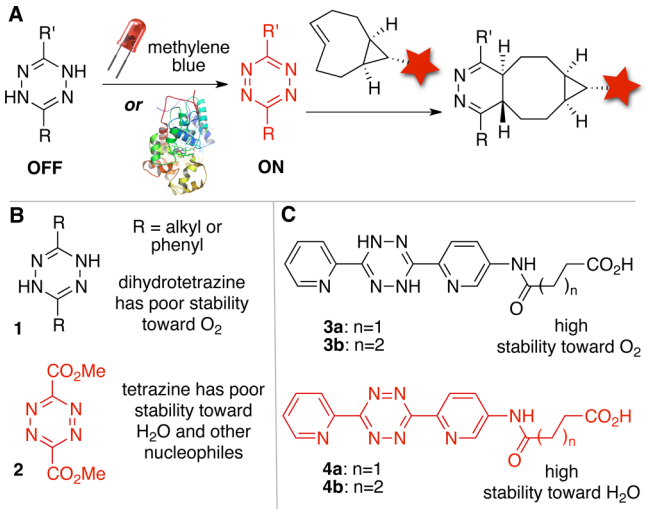

Figure 1. (A) Catalytic turn-on of tetrazine ligation. (B) Most dihydrotetrazine/tetrazine pairs have stability issues. (C) Identification of a dihydrotetrazine/tetrazine pair with high stability.

RESULTS AND DISCUSSION

A challenge to the development of catalytic methods for turning on the tetrazine ligation was the identification of a DHTz/Tz pair that would be stable in both oxidation states (Figure 1B). For most redox couples, either the DHTz is too readily oxidized in air (e.g., **1**), or the Tz is too reactive toward water and other nucleophiles (e.g., **2**). We show here that the dipyridyl DHTz/Tz pair[38] (**3**/**4**) has good stability in both states (Figure 1C). Dihydrotetrazines **3** are highly resilient toward background oxidation in organic solvents, and a number of derivatives have been synthesized and shown to be stable even to silica gel chromatography. In ambient light, a 35 μM solution of **3a** in MeOH was shown to retain 99% and 98% of the DHTz oxidation state after 1 and 2 h, respectively (Figure S10c). Aqueous solutions of **3a** were handled in glassware that had been first rinsed with 2.0 mM EDTA in PBS to remove adventitious metal impurities. After standing in the dark at 25 °C in PBS buffer, a solution of **3a** was monitored by UV−vis and shown to retain 99% and 96% of the DHTz oxidation state over 30 min and 2.5 h respectively (Figure S10a). In ambient light at 25 °C in PBS buffer, a solution of **3a** was shown to retain 97% and 94% of the DHTz oxidation state after 1 and 2 h, respectively (Figure S10d). In PBS containing 10% mouse serum, 90% of **3a** was retained in the DHTz oxidation state after 1 h (Figure S10f). Analogs of tetrazines **4** have been described previously and used broadly for applications in nuclear medicine and cell imaging.[31,39−43] In PBS buffer at 25 °C, tetrazine **4a** (800 μM) shows 98% and 83% fidelity after 2 and 24 h, respectively (Figure S11). The stability of a radiolabeled derivative of tetrazine **4b** has been studied by Robillard at 37 °C in PBS, serum, and blood, with 97%, 87%, and 59% retention of the tetrazine observed after 2 h.[41]

Compound **3a** has a maximum in the UV−vis spectrum at 292 nm, and **4a** has a maximum at 325 nm with a less intense peak at 525 nm (Figure 2). As a reference for our catalytic

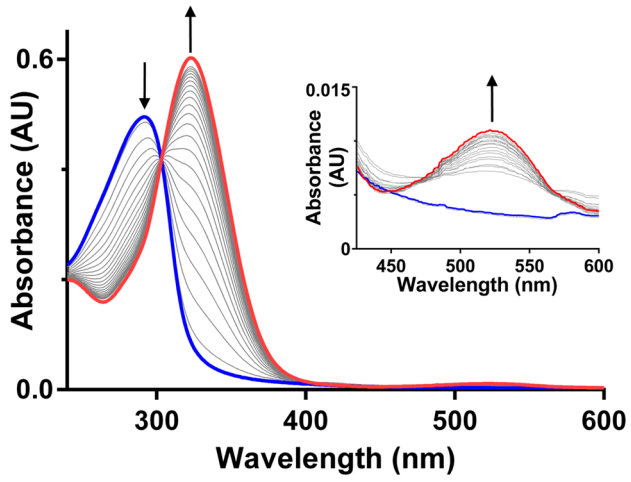

Figure 2. Compound **3a** (17 μM in PBS, blue spectrum) displays a maximum in the UV−vis spectrum at 292 nm. Compound **4a** (red spectrum) displays a maximum at 325 nm and a less intense peak at 525 nm (see inset). Upon addition of horseradish peroxidase (15 nM) the UV−vis spectrum was monitored every 10 s. With 50% conversion after 100 s, complete conversion of **3a** to **4a** is observed after 600 s, as evidenced by the decrease in the absorption at 292 nm and increase at 325 nm with an isosbestic point at 303 nm. Similar spectral changes are observed when **3a** is electrochemically oxidized to **4a** in aqueous solution, or when the oxidation of **3a** to **4a** is photocatalyzed by methylene blue.

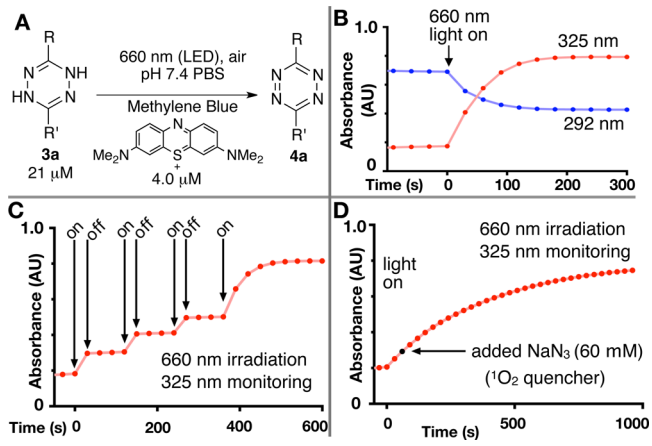

Figure 3. (A) Methylene blue catalyzed photooxidation of **3a** to **4a** was carried out with UV−vis monitoring and irradiation by a single LED centered at 660 nm. (B) After the onset of irradiation, reaction progress was monitored every 30 s at 325 nm, which increased with formation of **4a**, and 292 nm, which decreased upon consumption of **3a**. (C) The reaction progress requires irradiation and stalls when the LED is turned off. (D) The addition of 60 mM NaN_3, a singlet oxygen quencher, does not significantly slow the rate of conversion of **3a** to **4a**. In this experiment, the lamp intensity was reduced relative to experiments displayed in B and C.

DOI: 10.1021/jacs.6b02168
J. Am. Chem. Soc. 2016, 138, 5978−5983

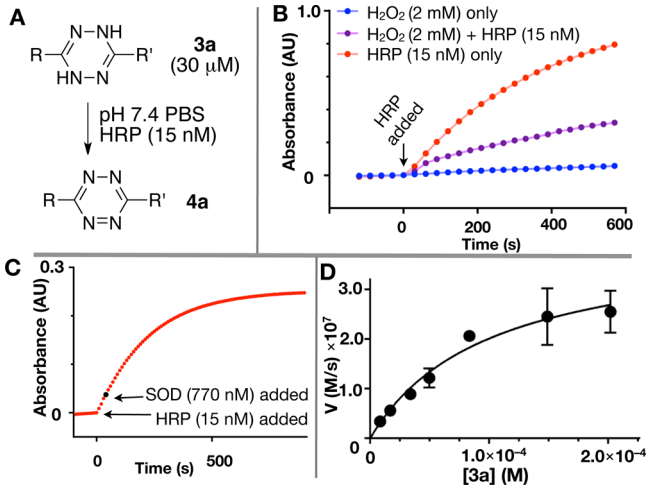

Figure 4. (A) Horseradish peroxidase catalyzed oxidation of **3a** to **4a**. Reactions were monitored by UV−vis every 30 s at 325 nm. (B) Enzymatic oxidation is most efficient in the absence of peroxide and is suppressed upon addition of peroxide. Hydrogen peroxide without catalyst is not an effective oxidant of **3a**. (C) The addition of superoxide dismutase does not suppress the rate of the oxidation of **3a** by HRP, providing evidence that superoxide is not responsible for the oxidation. (D) The oxidation of **3a** by HRP follows Michaelis−Menten kinetics. The reactions in (B, C) were carried out in PBS, and the reaction in (D) was carried out in PBS containing EDTA (2.0 mM).

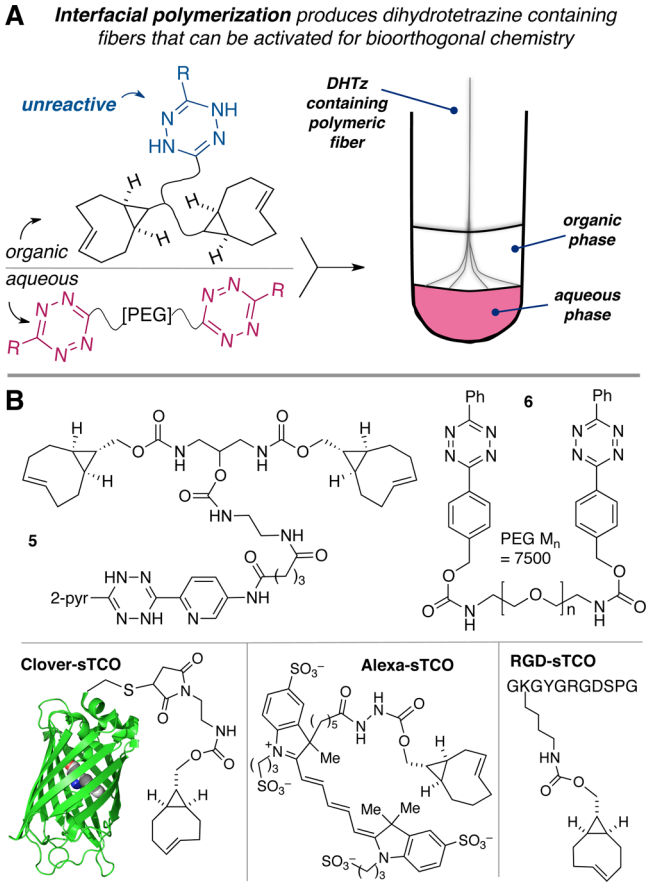

Figure 5. (A) Schematic representation of interfacial polymerization with a dihydrotetrazine-derived monomer. (B) Monomers **5** and **6** were used for interfacial polymerization. sTCO conjugates of the green fluorescent protein variant Clover, the dye Alexafluor 647, and an RGD peptide were used to modify the fibers.

studies, we first monitored the electrochemical oxidation of **3a** in phosphate buffer, for which the voltammogram displays a single peak centered at 0.02 V (Figure S13B). Under mildly oxidizing conditions (0.18 V relative to Ag/AgCl), a 1.1 mM solution of **3a** turns pink (Figure S13A) and the oxidation to **4a** proceeds cleanly with an isosbestic point at 303 nm (Figure S13C). This isosbestic point was also conserved in the photocatalytic (Figure S5) and enzymatic (Figure 2) oxidations of **3a** described below, and the spectroscopic changes at 292 and 325 nm were routinely used for monitoring reaction progress.

A number of photosensitizers in the presence of long wavelength visible light were found to catalyze the oxidation of **3a** to **4a** in the presence of air.[44] Methylene blue was considered a particularly attractive sensitizer due to its clinical relevance, low molecular weight, low toxicity, high solubility, and an absorption spectrum (λ_{max} 665 nm) that extends to the near-IR.[45] Further, methylene blue has previously been explored for applications in photodynamic therapy based on oxidation of indole-3-acetic acid.[46] Rose bengal (λ_{max} 550 nm), used in a range of biomedical applications, was also identified as an excellent sensitizer. Experiments to study the catalytic photooxidation were conducted at 25 °C in a thermostated cuvette with stirring capability and a single top-mounted LED. A custom 3D printed light fixture was used to mount the LED directly above the cuvette and block ambient light (Figure S4). As shown in Figure 3B, irradiation of **3a** (21 μM) with a 660 nm LED (9.1 mW/cm^2) in the presence of methylene blue (4 μM) in pH 7.4 PBS caused conversion to tetrazine **4a** with quantitative yield within 200 s. Methylene blue (4 μM) also catalyzed the conversion of **3a** to **4a** in the presence of ambient light, with 47% conversion noted after 2 h (Figure S10e). The light dependence of the methylene blue catalyzed oxidation was demonstrated by turning the LED on and off (Figure 3C). Similar light dependent on/off behavior was exhibited with either rose bengal or carboxyfluorescein with irradiation centered at 528 nm (2.3 mW/cm^2, Figures S8, S6). Both methylene blue and rose bengal are known $^1O_2$ sensitizers, and we therefore queried the influence of a $^1O_2$ quencher on the oxidation rate of **3a**. Neither the methylene blue (Figure 3D) nor the rose bengal (Figure S9) catalyzed photooxidations are impeded by the addition of 60 mM NaN_3. By contrast, the rate of the reaction between 2,5-diphenylisofuran with $^1O_2$ was greatly reduced when 23 mM NaN_3 was added (Figure S12). These experiments strongly imply that $^1O_2$ is not the oxidant of **3a** under photocatalytic conditions. The mechanism of photooxidation more likely involves electron transfer and is the subject of ongoing study.

As a complement to these photocatalyzed reactions, we observed that HRP can efficiently catalyze the oxidation of **3a** in the dark at low enzyme concentration (15 nM) (Figure 4). While HRP typically requires H_2O_2 as the terminal oxidant, the addition of HRP to a *peroxide-free* solution of **3a** (30 μM) in PBS led to the rapid formation of **4a** (Figure 4B). The rate of formation of **4a** was significantly slower in the presence of 2 mM H_2O_2 and was near baseline in the presence of H_2O_2 but absence of HRP. Neither cytochrome *c* nor hemoglobin were effective catalysts of DHTz oxidation, with only slow conversion of **3a** to **4a** even with heme concentrations that were nearly 3 orders of magnitude higher than that used with HRP (Figure S10b). As shown in Figure 4C, the addition of

DOI: 10.1021/jacs.6b02168
J. Am. Chem. Soc. 2016, 138, 5978−5983

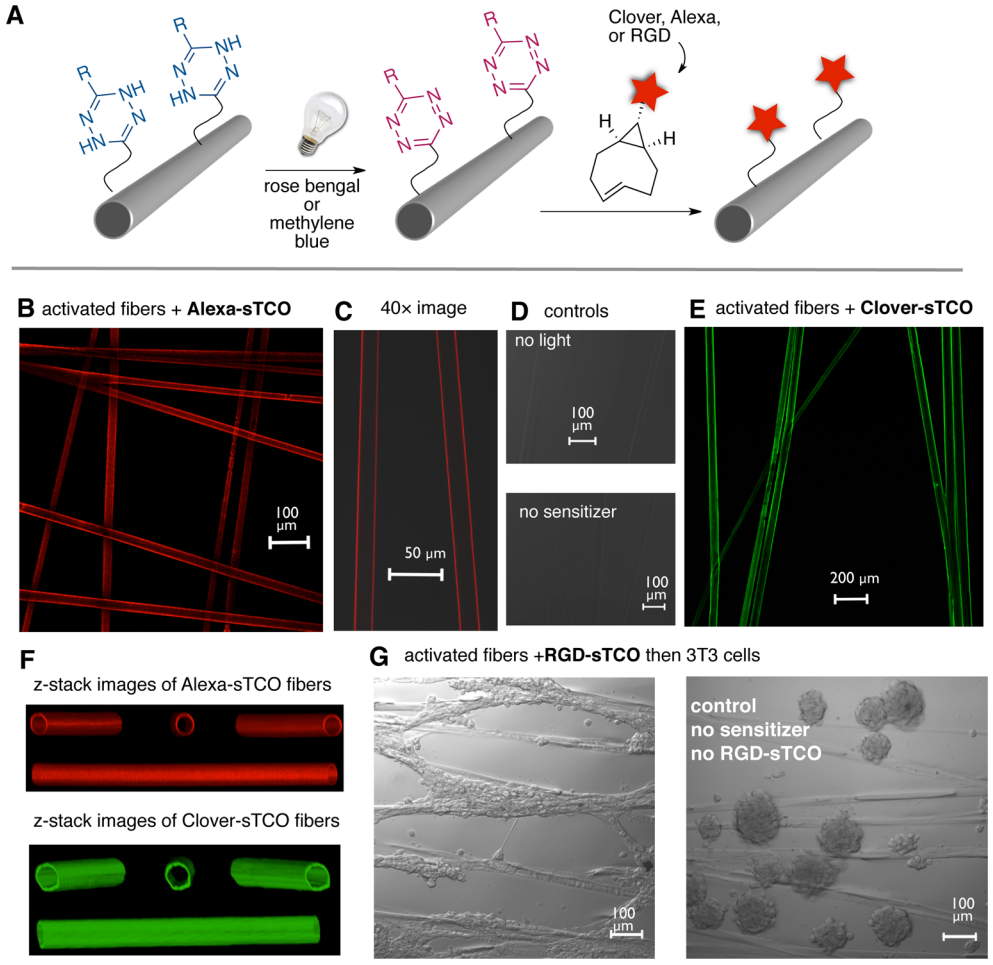

Figure 6. (A) Schematic representation of fiber photoactivation and subsequent conjugation. DHTz-containing fibers were isolated in a silicone well on a glass substrate (for imaging) or in a polyHEMA coated Nunc chamber (for cell culture). The fibers were immersed in a PBS solution of sensitizer (100 μM), irradiated with visible light for 5 min, rinsed, allowed to react with an sTCO conjugate, and again rinsed. (B,C) Confocal images (10×, 40×) of activated fibers (rose bengal) that were treated with Alexa-sTCO (1 μM) for 1 min and rinsed. (D) Tagging by Alexa-sTCO was not observed in control experiments where (top) the rose bengal was excluded, and (bottom) where the sensitizer was included, but light was excluded. (E) Confocal (10×) image of activated fibers (methylene blue) that were treated with Clover-sTCO (5 μM) for 1 min and rinsed. (F) Confocal z-stack images of activated fibers that were conjugated with Alexa-sTCO (top) and Clover-sTCO (bottom). (G) Confocal images (10×) of activated fibers (methylene blue) that were treated with RGD-sTCO (10 μM). Cell culture with NIH 3T3 fibroblasts for 20 h showed that the cells selectively adhered and spread on the fibers. Cell attachment and spreading on the fibers was not observed in control experiments where the sensitizer and/or the RGD-sTCO was excluded. The image above shows the control where both sensitizer and RGD-sTCO were excluded. Displayed in the Supporting Information are images from controls where only sensitizer was excluded, or where only RGD-sTCO was excluded.

superoxide dismutase (SOD, 770 nM) does not suppress the rate of the oxidation of **3a** by HRP, providing evidence that superoxide is not responsible for the oxidation. Finally, it was observed that the oxidation of **3a** by HRP follows Michaelis–Menten kinetics, with K_m = 1.0 × 10^{-4} M, k_{cat} = 27 s^{-1}, and k_{cat}/K_m = 2.7 × 10^5 M^{-1} s^{-1} (Figure 4D).

The light and enzyme-catalyzed reactions developed here enable the functionalization of polymeric materials with potential biomedical applications. We previously demonstrated the production of peptide-containing polymer fibers through interfacial bioorthogonal polymerization based on tetrazine ligation using bis-tetrazine and bis-TCO monomers dissolved in immiscible solvents.[47] These hydrogel-like polymer fibers, with diameters ranging from 6 to 11 μm when dry, are cytocompatible, biologically active, and mechanically robust; they resemble many fibrous structures found in the human body and can be woven into complex, higher order assemblies for tissue engineering purposes. However, the use of interfacial polymerization to fabricate protein-containing polymer fibers is not trivial due to the possibility of protein denaturation by the required organic solvent.

We hypothesized that fibers could be synthesized with latent dihydrotetrazines and, subsequently, be activated and functionalized through bioconjugation. Thus, an aqueous solution of a water-soluble bis-tetrazine monomer was combined with an organic soluble bis-sTCO containing a tethered dihydrotetrazine (Figure 5A). Again, meter-long, mechanically robust polymer fibers were continuously pulled from the liquid–liquid interface without fiber breakage (Video 1), confirming that the molecular weight of the polymer exceeds that required for chain entanglement.[47] Subsequent oxidation by long wavelength photocatalysis was used to generate reactive tetrazine functionality, and the fibers could then be functionalized by sTCO conjugates of proteins, fluorophores, or peptides. Shown in Figure 5B are the monomers **5** and **6** that were used to create the DHTz fibers. Notably, the DHTz containing bis-sTCO **5**

DOI: 10.1021/jacs.6b02168
J. Am. Chem. Soc. 2016, 138, 5978–5983

was readily purified, stored, and handled without special precautions. The sTCO conjugates used to elaborate the fibers are displayed in Figure 5B.

As shown in Figure 6, the DHTz-fibers could be activated and then postsynthetically modified by treatment with Alexa-sTCO, Clover[48]-sTCO, or RGD-sTCO. The fibers were immersed in 100 μM sensitizer in PBS and irradiated with a simple incandescent bulb for 5 min. Methylene blue was used to activate fibers toward conjugations of Clover-sTCO or RGD-sTCO, and rose bengal was used as the sensitizer in experiments with Alexa-sTCO due to the spectral overlap of the Alexa dye with methylene blue. After irradiation, the fibers were rinsed, allowed to react with an sTCO conjugate for 1 min, and rinsed again. Confocal microscopy images of activated fibers that were conjugated by Alexa-sTCO are displayed in Figure 6B and 6C. With this short incubation time, labeling was localized to the exterior of the fibers as clearly illustrated by the confocal z-stack images of the Clover-sTCO labeled fibers (Figure 6F, S19−20, Video 2) and Alexa-sTCO labeled fibers (Figures 6F, S14−15, Video 3). Control experiments illustrated that dye conjugation was not efficient if the sensitizer or light was excluded (Figures 6D, S16−18, S21−22). We note that HRP-catalyzed oxidation of dihydrotetrazines can also be used to activate fibers toward bioconjugation (Figure S23); however, in this instance photocatalytic activation is faster and more efficient.

The photocatalytic activation of tetrazines was also employed in the postsynthetic modification of the fibers with peptidic cues that promote cell adhesion and contact guidance. RGD-sTCO was conjugated to activated fibers through tetrazine ligation, and the resulting fibers were immobilized in silicone wells coated with poly(2-hydroxyethyl methacrylate) to eliminate cellular adhesion to the culture wells. Here, fibroblasts selectively attached to RGD-tagged fibers and elongated along the long axis of the fibers, adopting a healthy fibroblastic morphology (Figure 6G). Cell attachment and spreading was not observed in control experiments where the sensitizer and/or the RGD-sTCO were excluded (Figures 6G, S26−S28). Instead, cells clustered to form multicellular spheroids, indicating the initiation of nemesis.[49] These studies demonstrate the ability to functionalize biomimetic fibers with molecules that can enable visualization or promote cell adhesion.

As shown here, photocatalytic and enzymatic methods for turning on the tetrazine ligation provide a new tool for modulating the cell adhesive properties of a biomaterial. With future development we expect that the catalytically inducible tetrazine ligation will extend to a wide range of applications in materials, cellular, and *in vivo* systems. We also expect that the electrochemical oxidation of dihydrotetrazines in solution will serve as an important stimulus for inducing bioorthogonal reactivity. We further anticipate that the new methods for inducing rapid bioorthogonal chemistry presented here should find a range of applications including cell imaging, pretargeted prodrug activation, and gene activation.

■ ASSOCIATED CONTENT

Supporting Information

The Supporting Information is available free of charge on the ACS Publications website at DOI: 10.1021/jacs.6b02168.

Synthetic procedures and compound characterization data; procedures for dihydrotetrazine (DHTz) and DHTz-containing microfiber oxidation/tagging experiments; confocal microscopic images of DHTz-containing microfiber tagging experiments and NIH 3T3 fibroblast cell attachment experiments (PDF)

Web-Enhanced Features

A video showing meter-long polymer fibers being pulled from a liquid−liquid interface without breakage and videos illustrating Clover-sTCO and Alexa-sTCO labeled fibers in MOV format are availabe in the online version of the paper.

■ AUTHOR INFORMATION

Corresponding Author

*jmfox@udel.edu

Author Contributions

§H.Z. and W.S.T. contributed equally.

Notes

The authors declare no competing financial interest.

■ ACKNOWLEDGMENTS

For funding this research, we are grateful to NSF DMR-1506613, NIH DC014461, NIH GM26643, P20GM104316, and the Osteoscience Foundation. K.T.D. is grateful for a Robert Gore Fellowship. Spectra were obtained with instrumentation supported by NIH Grants P20GM104316, P30GM110758, S10RR026962, S10OD016267 and NSF Grants CHE-0840401, CHE-1229234.

■ REFERENCES

(1) Sletten, E. M.; Bertozzi, C. R. *Angew. Chem., Int. Ed.* **2009**, *48*, 6974.
(2) Lang, K.; Chin, J. W. *Chem. Rev.* **2014**, *114*, 4764.
(3) Azagarsamy, M. A.; Anseth, K. S. *ACS Macro Lett.* **2013**, *2*, 5.
(4) McKay, C. S.; Finn, M. G. *Chem. Biol.* **2014**, *21*, 1075.
(5) Jewett, J. C.; Bertozzi, C. R. *Chem. Soc. Rev.* **2010**, *39*, 1272.
(6) Shih, H.-W.; Kamber, D. N.; Prescher, J. A. *Curr. Opin. Chem. Biol.* **2014**, *21*, 103.
(7) MacKenzie, D. A.; Sherratt, A. R.; Chigrinova, M.; Cheung, L. L. W.; Pezacki, J. P. *Curr. Opin. Chem. Biol.* **2014**, *21*, 81.
(8) Yu, Z.; Ohulchanskyy, T. Y.; An, P.; Prasad, P. N.; Lin, Q. *J. Am. Chem. Soc.* **2013**, *135*, 16766.
(9) Tasdelen, M. A.; Yagci, Y. *Angew. Chem., Int. Ed.* **2013**, *52*, 5930.
(10) Ramil, C. P.; Lin, Q. *Curr. Opin. Chem. Biol.* **2014**, *21*, 89.
(11) Arumugam, S.; Orski, S. V.; Mbua, N. E.; McNitt, C.; Boons, G.-J.; Locklin, J.; Popik, V. V. *Pure Appl. Chem.* **2013**, *85*, 1499.
(12) Debets, M. F.; van Berkel, S. S.; Dommerholt, J.; Dirks, A. T. J.; Rutjes, F. P. J. T.; van Delft, F. L. *Acc. Chem. Res.* **2011**, *44*, 805.
(13) Versteegen, R. M.; Rossin, R.; ten Hoeve, W.; Janssen, H. M.; Robillard, M. S. *Angew. Chem., Int. Ed.* **2013**, *52*, 14112.
(14) Matikonda, S. S.; Orsi, D. L.; Staudacher, V.; Jenkins, I. A.; Fiedler, F.; Chen, J.; Gamble, A. B. *Chem. Sci.* **2015**, *6*, 1212.
(15) Li, J.; Jia, S.; Chen, P. R. *Nat. Chem. Biol.* **2014**, *10*, 1003.
(16) Grim, J. C.; Marozas, I. A.; Anseth, K. S. *J. Controlled Release* **2015**, *219*, 95.
(17) Urdabayev, N. K.; Poloukhtine, A.; Popik, V. V. *Chem. Commun.* **2006**, 454.
(18) Dore, T. D.; Wilson, H. C. In *Chromophores for the Delivery of Bioactive Molecules with Two-Photon Excitation*; Chambers, J. J., Kramer, R. H., Eds.; Neuromethods; Humana Press: Totowa, NJ, 2011; Vol. *55*, pp 57−92.
(19) Gorka, A. P.; Nani, R. R.; Zhu, J.; Mackem, S.; Schnermann, M. J. *J. Am. Chem. Soc.* **2014**, *136*, 14153.
(20) Palao, E.; Slanina, T.; Muchová, L.; Šolomek, T.; Vítek, L.; Klán, P. *J. Am. Chem. Soc.* **2016**, *138*, 126.
(21) Nkepang, G.; Bio, M.; Rajaputra, P.; Awuah, S. G.; You, Y. *Bioconjugate Chem.* **2014**, *25*, 2175.

DOI: 10.1021/jacs.6b02168
J. Am. Chem. Soc. 2016, 138, 5978−5983

(22) Olejniczak, J.; Carling, C.-J.; Almutairi, A. *J. Controlled Release* **2015**, *219*, 18.
(23) Ritter, C.; Nett, N.; Acevedo-Rocha, C. G.; Lonsdale, R.; Kräling, K.; Dempwolff, F.; Hoebenreich, S.; Graumann, P. L.; Reetz, M. T.; Meggers, E. *Angew. Chem., Int. Ed.* **2015**, *54*, 13440.
(24) Azevedo, A. M.; Martins, V. C.; Prazeres, D. M. F.; Vojinović, V.; Cabral, J. M. S.; Fonseca, L. P. *Biotechnol. Annu. Rev.* **2003**, *9*, 199.
(25) Wardman, P. *Curr. Pharm. Des.* **2002**, *8*, 1363.
(26) Folkes, L. K.; Wardman, P. *Biochem. Pharmacol.* **2001**, *61*, 129.
(27) Klapper, M. H.; Hackett, D. P. *J. Biol. Chem.* **1963**, *238*, 3736.
(28) Yokota, K.; Yamazaki, I. *Biochemistry* **1977**, *16*, 1913.
(29) Wu, H.; Devaraj, N. K. *Top. Curr. Chem.* **2016**, *374*, 3.
(30) Devaraj, N. K.; Weissleder, R. *Acc. Chem. Res.* **2011**, *44*, 816.
(31) Selvaraj, R.; Fox, J. M. *Curr. Opin. Chem. Biol.* **2013**, *17*, 753.
(32) Darko, A.; Wallace, S.; Dmitrenko, O.; Machovina, M. M.; Mehl, R. A.; Chin, J. W.; Fox, J. M. *Chem. Sci.* **2014**, *5*, 3770.
(33) Taylor, M. T.; Blackman, M. L.; Dmitrenko, O.; Fox, J. M. *J. Am. Chem. Soc.* **2011**, *133*, 9646.
(34) Selvaraj, R.; Fox, J. M. *Tetrahedron Lett.* **2014**, *55*, 4795.
(35) Clavier, G.; Audebert, P. *Chem. Rev.* **2010**, *110*, 3299.
(36) Ehret, F.; Wu, H.; Alexander, S. C.; Devaraj, N. K. *J. Am. Chem. Soc.* **2015**, *137*, 8876.
(37) Nickerl, G.; Senkovska, I.; Kaskel, S. *Chem. Commun. (Cambridge, U. K.)* **2015**, *51*, 2280.
(38) Blackman, M. L.; Royzen, M.; Fox, J. M. *J. Am. Chem. Soc.* **2008**, *130*, 13518.
(39) Lang, K.; Davis, L.; Wallace, S.; Mahesh, M.; Cox, D. J.; Blackman, M. L.; Fox, J. M.; Chin, J. W. *J. Am. Chem. Soc.* **2012**, *134*, 10317.
(40) Rossin, R.; van den Bosch, S. M.; Ten Hoeve, W.; Carvelli, M.; Versteegen, R. M.; Lub, J.; Robillard, M. S. *Bioconjugate Chem.* **2013**, *24*, 1210.
(41) Rossin, R.; Renart Verkerk, P.; van den Bosch, S. M.; Vulders, R. C. M.; Verel, I.; Lub, J.; Robillard, M. S. *Angew. Chem., Int. Ed.* **2010**, *49*, 3375.
(42) Wu, Z.; Liu, S.; Hassink, M.; Nair, I.; Park, R.; Li, L.; Todorov, I.; Fox, J. M.; Li, Z.; Shively, J. E.; Conti, P. S.; Kandeel, F. *J. Nucl. Med.* **2013**, *54*, 244.
(43) Rossin, R.; Robillard, M. S. *Curr. Opin. Chem. Biol.* **2014**, *21*, 161.
(44) Other successful sensitizers (irradiation wavelength) include acridine orange (528 nm), coomassie brilliant blue (528 nm), rhodamine B (590 nm), BODIPY (475 nm), safranin (528 nm), phenol red (528 nm), and carboxylfluorescein (528 nm).
(45) Schirmer, R. H.; Adler, H.; Pickhardt, M.; Mandelkow, E. *Neurobiol. Aging* **2011**, *32*, 2325.e7.
(46) Folkes, L. K.; Wardman, P. *Cancer Res.* **2003**, *63*, 776.
(47) Liu, S.; Zhang, H.; Remy, R. A.; Deng, F.; Mackay, M. E.; Fox, J. M.; Jia, X. *Adv. Mater.* **2015**, *27*, 2783.
(48) Lam, A. J.; St-Pierre, F.; Gong, Y.; Marshall, J. D.; Cranfill, P. J.; Baird, M. A.; McKeown, M. R.; Wiedenmann, J.; Davidson, M. W.; Schnitzer, M. J.; Tsien, R. Y.; Lin, M. Z. *Nat. Methods* **2012**, *9*, 1005.
(49) Salmenperä, P.; Kankuri, E.; Bizik, J.; Sirén, V.; Virtanen, I.; Takahashi, S.; Leiss, M.; Fässler, R.; Vaheri, A. *Exp. Cell Res.* **2008**, *314*, 3444.

DOI: 10.1021/jacs.6b02168
J. Am. Chem. Soc. 2016, 138, 5978−5983